Desalination and Water Treatment
www.deswater.com

doi: 10.1080/19443994.2014.979446

57 (2016) 2006–2017
January

Taylor & Francis
Taylor & Francis Group

Optimization of lead (II) sorption potential using developed activated carbon from tamarind wood with chemical activation by zinc chloride

J.N. Sahu[a,b,1,*], Jyotikusum Acharya[c], B.K. Sahoo[a], B.C. Meikap[a,d]

[a] *Department of Chemical Engineering, Indian Institute of Technology (IIT), P.O. Kharagpur Technology, Kharagpur 721302, West Bengal, India, Tel. +603 7967 5295; Fax: +603 7967 5319; email: jay_sahu@yahoo.co.in (J.N. Sahu)*
[b] *Faculty of Engineering, Department of Chemical Engineering, University of Malaya, Kuala Lumpur 50603, Malaysia*
[c] *Department of Civil Engineering, National Institute of Technology, Silchar 788010, Assam, India*
[d] *Faculty of Engineering, School of Chemical Engineering, University of KwaZulu-Natal, Howard College Campus, King George V. Avenue, Durban 4041, South Africa*

Received 22 March 2014; Accepted 17 October 2014

ABSTRACT

An adsorbent prepared from tamarind wood with chemical activation by zinc chloride was used to study its sorption potential on removing lead (II). An efficient response surface methodology (RSM) is used for optimization of removal of lead (II) from aqua solutions. While the goal of adsorption of lead (II) optimization was to improve adsorption conditions in batch process, i.e. to minimize the adsorbent doses and to increase the initial concentrations of lead (II). A 2^4 full factorial central composite design experimental design was employed. Analysis of variance showed a high coefficient of determination value ($R^2 = 0.996$) and satisfactory prediction second-order regression model was derived. Maximum lead removal efficiency was predicted and experimentally validated. The optimum adsorbent dose, temperature, initial concentration of lead (II), and initial pH of the lead (II) solution were found to be 1.44 g L^{-1}, 50°C, 49.23 mg L^{-1}, and 4.07, respectively. Under optimal value of process parameters, high removal (>99%) was obtained for lead (II). The study clearly showed that RSM was one of the suitable methods to optimize the operating conditions and maximize the lead removal. Graphical response surface and contour plots were used to locate the optimum point.

Keywords: Adsorption; Activated carbon; Lead (II); Optimization; Tamarind wood; Wastewater treatment

1. Introduction

The major sources of containing lead are the wastewater from process industries engaged in lead-acid battery, paints, oils, metal, phosphate fertilizer, electronic components manufacture, wood production, and also combustion of fossil fuel, forest fires, mining activity, automobile emission, sewage wastewater, sea spray, etc. [1–3]. The industrial wastewaters are considered to be the main source of lead impurities.

---

*Corresponding author.

[1] Petroleum and Chemical Engineering Programme Area, Faculty of Engineering, Institut Teknologi Brunei, Tungku Gadong, P.O. Box 2909, Brunei Darussalam.

Lead is also present at 50 parts per million (ppm) in the earth's crust. In sea water, 5 parts per billion (ppb) lead is present. It is found in all living organisms. A human body contains about 121 ppb, 96% in the bone [4]. The concentration of lead increases with age, and it may reach to a limit at 400 mg. It is not essential for mammals. Under specific condition, lead is stimulatory causing enhancing of protein synthesis, DNA synthesis, and cell replication. Lead is deposited mostly in bones and in some soft tissues. It is also retaining by mammals in liver, kidney, muscles, etc. About 800 mg of lead create toxicity in human beings. It is systemic poison causing anemia, kidney malfunction, tissue damage of brain, and even death in extreme poison. Lead occurs as its sulfide, cerussite ($PbCl_2$), and galena.

The presence of high levels of lead in the environment may cause long-term health risks to humans and ecosystems. The presence of lead in wastewater is dangerous to aquatic flora and fauna even in relatively low concentration, and stringent environmental regulation attracts the attention of chemists and environmental engineers for its control. Increasingly, stringent legislation on the purity of drinking water has created a growing interest in the development of chemical and physico-chemical treatment processes.It is therefore mandatory that their levels in drinking water, wastewater, and water used for agricultural and recreational purposes must be reduced to within the maximum allowable concentrations recommended by national and international health authorities such as World Health Organisation, the permissible level for Pb in drinking water is 0.05 mg L^{-1} [5]. Its removal from wastewater prior to discharge into the environment is, therefore, necessary. Current EPA drinking water standard for lead are 0.05 mg L^{-1}, but a level of 0.02 mg L^{-1} has been proposed and is under review [6]. According to Indian Standard Institution, the tolerance limit for discharge of lead into drinking water is 0.05 mg L^{-1} [7] and in land surface waters is 0.1 mg L^{-1} [8]. Various chemical and physico-chemical methods for the treatment of wastewaters containing lead wastes are known, such as chemical precipitation, electrochemical reduction, ion exchange, biosorption, and adsorption [9–13]. The choice of treatment depends on effluent characteristics such as concentration of lead, pH, temperature, flow volume, biological oxygen demand, and the economics involved and the social factor like standard set by government agencies. However, adsorption on to the surface of activated carbons is the most widely used method [14–19].

Adsorption is a versatile treatment technique practiced widely in fine chemical and process industries for wastewater and waste gas treatment. The usefulness of the adsorption process lies in the operational simplicity and reuse potential of adsorbents during long-term applications. Carbon adsorption has proved to be the least expensive treatment option, particularly in treating low concentrations of wastewater streams and in meeting stringent treatment levels. Activated carbon is a black solid substance resembling granular or powder charcoal and is a carbonaceous material that has highly developed porosity, internal surface area, and relatively high mechanical strength. Activated carbon-based systems can remove a wide variety of toxic pollutants with very high removal efficiencies. For the reasons, activated carbon adsorption has been widely used for the treatment of lead containing wastewaters [14–19]. However, commercially available activated carbons may be expensive and, for the reason, the knowledge of the optimal working conditions to maximize the sorbent capture capacity is required. The materials developed for the purpose range from agricultural waste products, biomass, and various solid substances. Some examples are activated groundnut husk carbon, coconut husk and palm pressed fibers, coconut shell, wood and dust coal activated carbons, coconut tree sawdust carbon, used tyres carbon, rice husk carbon, hazelnut shell carbon, almond shell carbon, and maize tassel, have been reported in the literature [20–29].

In the work, it has been reported the results obtained on the preparation of activated carbon from tamarind wood with zinc chloride activation and their ability to remove lead (II) from wastewater. The influence of several operating parameters, such as initial concentration, temperature, pH, and adsorbent dose were investigated in batch mode. The published information in the literature about adsorption of lead in activated carbon is well detailed [14–19]. However, there is no information available in the literature regarding the optimization of lead adsorption on activated carbon. Therefore, we decided to study more thoroughly the phenomenon of adsorption of lead (II) in tamarind wood-activated carbon. The effects of operating parameters such as initial feed concentration, temperature, pH, and adsorbent dose were optimized using response surface methodology (RSM). The optimization of experimental conditions using RSM was widely applied in various processes [30–42]; however, its application in adsorption of lead (II) in tamarind wood-activated carbon was not available in the literature.

2. Materials and methods

2.1. *Adsorbate: Lead (II)*

A stock solution of lead (II) was prepared (1,000 mg L^{-1}) by dissolving required amount of Pb

$(NO_3)_2$ in distilled water. The stock solution was diluted with distilled water to obtain desired concentration ranging from 20 to 60 mg L^{-1}.

2.2. Adsorbent: Tamarind wood activated carbon

The tamarind wood was collected from local Indian Institute of Technology campus of Kharagpur, West Bengal, India and washed with deionized water four to five times for removing dirt and dust particles. The washed wood was cut into 50.8–76.2 mm pieces. The wood was sun dried for 20 d. Chemical activation of the precursor was done with $ZnCl_2$. Ten grams of dried precursor was well mixed with distilled water so that 100 ml concentrated solution contained 10 g of $ZnCl_2$. The chemical ratio is defined as the ratio of chemical activating agent ($ZnCl_2$) to the precursor. The chemical ratio (activating agent/precursor) was 100% in our case. The mixing was performed at 50℃ for 1 h. After mixing, the slurry was subjected to vacuum drying at 100℃ for 24 h. The resulting chemical-loaded samples were placed in a stainless steel tubular reactor and heated (5℃ min^{-1}) to the final carbonization temperature under a nitrogen flow rate of 150 mL min^{-1} STP. Samples were held at the final temperature (carbonization temperature) for carbonization times of 40 min before cooling down under nitrogen. Nitrogen entering into the reactor was first preheated to 250–300℃ in a preheater. In all experiments, heating rate and nitrogen flow were kept constant. The experiments were carried out for chemical ratio of (100%) and carbonization temperature (450℃). The products were washed sequentially with 0.5 N HCl, hot water, and finally cold distilled water to remove residual organic and mineral matters, and then dried at 110℃. After that, carbon was crushed in a small ball mill with 50 small balls for 1 h. The powder from ball mill is collected and dried to remove the moisture. Then, the powder carbon was kept in airtight packet for the experimental use.

2.3. Batch adsorption experiment

The experiments were performed in a thermal shaker at controlled temperature for a period of 1 h at 120 rpm using 250 mL Erlenmeyer flasks containing 100 mL of different lead (II) concentrations at different temperatures (10–50℃). The jar tests were carried out to study the effect of various operating variables on the adsorption rate. Adsorption of lead (II) on developed activated carbon was conducted containing different weighted amounts of each sample with 100 mL solution of different initial concentration of lead (II) ions. The batch process was used so that there is no need for volume correction. Samples were taken out at regular interval, and the residual concentration in the solution was analyzed using atomic absorption spectroscopy after filtering the adsorbent with Whatman filter paper to make it carbon free.

2.4. Experiment parameter

The effect of pH on the percentage removal was investigated over the range of 2–10. The pH was adjusted by the addition of 0.1 M HCl or NaOH. The effect of adsorbent dose (1–10 g L^{-1}), initial lead (II) ion concentration (10–100 mg L^{-1}), and temperature (10–50℃) on the adsorption potential of lead (II) ions was studied. The lead (II) concentration retained in the adsorbent phase was calculated according to:

$$q_e = \frac{(C_0 - C_e)V}{W} \tag{1}$$

where C_0 and C_e are the initial and equilibrium concentrations (mg L^{-1}) of lead (II) solution, respectively; V is the volume (L); and W is the weight (g) of the adsorbent.

By calculating the lead (II) concentration at initial concentrations and equilibrium concentrations, the efficiency of adsorption of lead by activated carbon can be calculated using the following equation for efficiency of adsorption lead (II):

$$\text{Adsorption}\,(\%) = \frac{C_0 - C_e}{C_0} \times 100 \tag{2}$$

2.5. Multivariate experimental design

RSM is a statistical method that uses quantitative data from appropriate experiments to determine regression model equations and operating conditions [30–34]. RSM is a collection of mathematical and statistical techniques for modeling and analysis of problems in which a response of interest is influenced by several variables [35]. A standard RSM design called central composite design (CCD) was applied in the work to study the variables for adsorption of lead from aqueous solution using prepared activated carbon in a batch process.

The CCD was widely used for fitting a second-order model. Using the method, modeling is possible and it requires only a minimum number of experiments. It is not necessary in the modeling procedure to know the detailed reaction mechanism since the mathematical model is empirical. Generally, the CCD consists of a 2^n factorial runs with $2n$ axial runs and n_c center runs (six replicates). The designs consist of a 2^n factorial or fractional (coded to the usual ±1 notation) augmented by $2n$ axial points $(\pm\alpha, 0, 0, \ldots, 0)$, $(0, \pm\alpha, 0, \ldots, 0)$, …, $(0, 0, \ldots, \pm\alpha)$, and n_c center points $(0, 0, 0, \ldots, 0)$ [36]. Each variable is investigated at two levels. Meanwhile, as the number of factors, n, increases, the number of runs for a complete replicate of the design increases rapidly. In the case, main effects and interactions may be estimated by fractional factorial designs running only a minimum number of experiments. Individual second-order effects cannot be estimated separately by 2^n factorial designs. Therefore, the CCD was employed in the study using our early study results on the nature of adsorption of lead (II) in detailed in previous experimental studies [19]. The responses and the corresponding parameters are modeled, and optimized lead (II) adsorption variables using analysis of variance (ANOVA), also ANOVA used to estimate the statistical parameters by means of response surface methods.

Basically, the optimization process involves three major steps, which are, performing the statistically designed experiments, estimating the coefficients in a mathematical model, and predicting the response and checking the adequacy of the model.

$$Y = f(X_1, X_2, X_3, X_4 \ldots X_n) \qquad (3)$$

where Y is the response of the system and X_i is the variables of action called factors. The goal is to optimize the response variable (Y). It is assumed that the independent variables are continuous and controllable by experiments with negligible errors. It is required to find a suitable approximation for the true functional relationship between independent variables and the response surface [37].

The true relationship between Y and X_n may be complicated and, in most cases, it is unknown. In the case, by assuming high-order interactions negligible, main effects and low-order interactions may be estimated by fractional factorial designs. Individual second-order effects cannot be estimated separately by 2^n factorial designs. The first order model is as follows:

$$Y = b_0 + \sum_{i=1}^{n} b_i X_i + \sum_{i}^{n} \sum_{j}^{n} b_{ij} X_i X_j \qquad (4)$$

The four independent variables X_1, X_2, X_3, and X_4 and the mathematical relationship of the response Y on the variables can be approximated by quadratic/(second degree) polynomial Eq. (5) as shown below:

$$\begin{aligned} Y = {} & b_0 + b_1X_1 + b_2X_2 + b_3X_3 + b_4X_4 + b_{12}X_1X_2 \\ & + b_{13}X_1X_3 + b_{14}X_1X_4 + b_{23}X_2X_3 + b_{24}X_2X_4 \\ & + b_{34}X_3X_4 + b_{11}X_1^2 + b_{22}X_2^2 + b_{33}X_3^2 + b_{44}X_4^2 \end{aligned} \qquad (5)$$

where b_0 the constant, b_1, b_2, b_3, and b_4 the linear coefficients, b_{12}, b_{13}, b_{14}, b_{23}, b_{24}, and b_{34} the cross product coefficients, and b_{11}, b_{22}, b_{33}, and b_{44} are the quadratic coefficients.

The number of tests required for the CCD includes the standard 2^n factorial with its origin at the center, $2n$ points fixed axially at a distance, say α from the center to generate the quadratic terms, and replicate tests at the center; where n is the number of variables. The axial points are chosen such that they allow rotatability [38], which ensures that the variance of the model prediction is constant at all points equidistant from the design center. Replicates of the test at the center are very important as they provide an independent estimate of the experimental error. For four variables, the recommended number of tests at the center is six [39]. Hence, the total number of tests (N) required for the four independent variables is:

$$N = 2^n + 2n + n_c = 2^4 + (2 \times 4) + 6 = 30 \qquad (6)$$

Once the desired range of values of the variables are defined, they are coded to lie at ±1 for the factorial points, 0 for the center points and $\pm\alpha$ for the axial points. The codes are calculated as functions of the range of interest of each factor as shown in Table 1 [40].

3. Results and discussion

3.1. Development of regression model equation

CCD was used to develop correlation between the adsorption of lead (II) from aqueous solution variables to the adsorption of lead (II) in activated carbon. The complete experimental range and levels of independent variables are given in Table 2. Runs 25–30 at the center point were used to determine the experimental error. According to the sequential model sum of squares, the models were selected based on

Table 1
Relationship between coded and actual value of the variables

Code	Actual level of variable
$-\alpha$	$X_{\min}$
−1	$[(X_{\max} + X_{\min})/2] - [(X_{\max} - X_{\min})/2\beta]$
0	$(X_{\max} + X_{\min})/2$
+1	$[(X_{\max} + X_{\min})/2] + [(X_{\max} - X_{\min})/2\beta]$
$+\alpha$	$X_{\max}$

where $X_{\max}$ and $X_{\min}$ are maximum and minimum values of X, respectively; β is $2^{n/4}$.

the highest order polynomials where the additional terms were significant and the models were not aliased. The quadratic model was selected as suggested by the software. Experiments were planned to obtain a quadratic model consisting of 2^4 trials plus a star configuration ($\alpha = \pm 2$) and there replicates at the center point. The design of the experiment is given in Table 3, together with the experimental results. The maximum adsorption of lead (II) was found to be $>96\%$. Regression analysis was performed to fit the response function of adsorption of lead (%). The model expressed by Eq. (5), where the variables take their coded values, represents adsorption (Y) as a function of temperatures (X_1), pH (X_2), initial feed concentrations

Table 2
Experimental range and levels of independent variables

Variables	Symbol	$-\alpha$	−1	0	+1	$+\alpha$
Temperature (°C)	X_1	10	20	30	40	50
pH	X_2	2	4	6	8	10
Initial concentration (mg L^{-1})	X_3	10	20	30	40	50
Adsorbent dose (g L^{-1})	X_4	1	2	3	4	5

Table 3
Experimental design matrix and results

	Coded level of variables				Actual level of variables				
Run	X_1	X_2	X_3	X_4	X_1 (°C)	X_2	X_3 (mg L^{-1})	X_4 (g L^{-1})	Adsorption experimental, Y (%)
1	−1	−1	−1	−1	20	4	20	2	66.25
2	+1	−1	−1	−1	40	4	20	2	76.42
3	−1	+1	−1	−1	20	8	20	2	84.04
4	+1	+1	−1	−1	40	8	20	2	93.68
5	−1	−1	+1	−1	20	4	40	2	75.35
6	+1	−1	+1	−1	40	4	40	2	79.49
7	−1	+1	+1	−1	20	8	40	2	82.22
8	+1	+1	+1	−1	40	8	40	2	84.26
9	−1	−1	−1	+1	20	4	20	4	86.38
10	+1	−1	−1	+1	40	4	20	4	91.18
11	−1	+1	−1	+1	20	8	20	4	90.84
12	+1	+1	−1	+1	40	8	20	4	96.24
13	−1	−1	+1	+1	20	4	40	4	82.46
14	+1	−1	+1	+1	40	4	40	4	82.32
15	−1	+1	+1	+1	20	8	40	4	79.34
16	+1	+1	+1	+1	40	8	40	4	78.65
17	0	0	0	$-\alpha$	10	6	30	3	83.93
18	0	0	0	$+\alpha$	50	6	30	3	93.80
19	0	0	$-\alpha$	0	30	2	30	3	62.72
20	0	0	$+\alpha$	0	30	10	30	3	73.57
21	0	$-\alpha$	0	0	30	6	10	3	96.91
22	0	$+\alpha$	0	0	30	6	50	3	85.36
23	$-\alpha$	0	0	0	30	6	30	1	78.03
24	$+\alpha$	0	0	0	30	6	30	5	90.26
25	0	0	0	0	30	6	30	3	78.60
26	0	0	0	0	30	6	30	3	78.56
27	0	0	0	0	30	6	30	3	78.66
28	0	0	0	0	30	6	30	3	78.63
29	0	0	0	0	30	6	30	3	78.60
30	0	0	0	0	30	6	30	3	78.56

of lead (II) (X_3) and adsorbent doses (X_4). The final empirical model in the terms of coded factors for the adsorption of lead (II) (Y) is shown in Eq. (7):

$$\begin{aligned} Y = {} & 78.61 + 2.30X_1 + 2.96X_2 - 2.67X_3 + 2.92X_4 \\ & - 0.16X_1X_2 - 1.54X_1X_3 - 1.04X_1X_4 - 2.48X_2X_3 \\ & - 2.75X_2X_4 - 2.67X_3X_4 + 2.57X_1^2 - 2.61X_2^2 \\ & + 3.13X_3^2 + 1.39X_4^2 \end{aligned} \tag{7}$$

3.2. Statistical analysis

Eq. (7) has been used to visualize the effects of experimental factors on conversion percentage response in Figs. 1–9. The model adequacy check is an important part of the data analysis procedure as the approximating model would give poor or misleading results if it were an inadequate fit. This is done by looking at the residual plots which are examined for the approximating model [41]. The normal probability and studentized residuals plot are shown in Fig. 1 for the adsorption of lead (II). In Fig. 1, residuals show how well the model satisfies the assumptions of the ANOVA whereas the studentized residuals measure the number of standard deviations separating the actual and predicted values. Fig. 1 shows that neither response transformation was needed nor there was any apparent problem with normality. Fig. 2 shows the studentized residuals versus predicted conversion percent. The general impression is that the plot should be a random scatter, suggesting the variance of original observations is constant for all values of the response. If the variance of the response depends on the mean level of Y, then the plot often exhibits a funnel-shaped pattern [42]. Here, it is also an indication that there was no need for transformation of the response variable.

The actual and the predicted adsorption of lead percent are shown in Fig. 3. Actual values are the measured response data for a particular run, and the

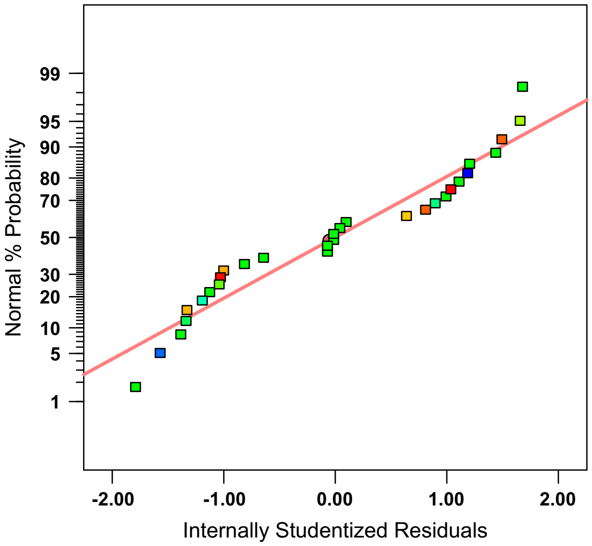

Fig. 1. The studentized residuals and normal percentage probability plot of adsorption of lead (II).

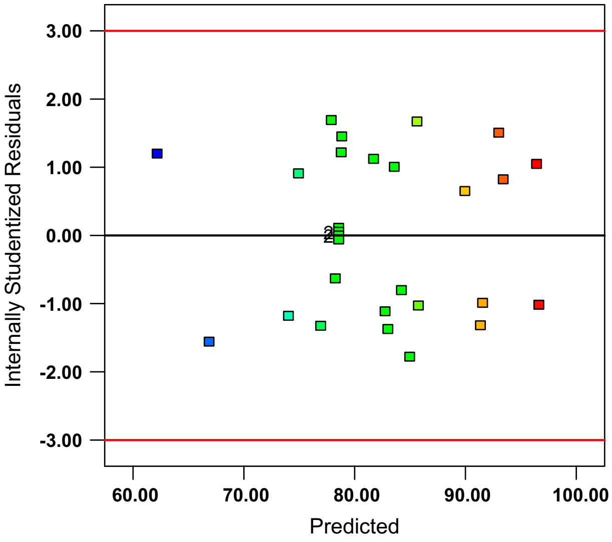

Fig. 2. The predicted adsorption of lead (II) and studentized residuals plot.

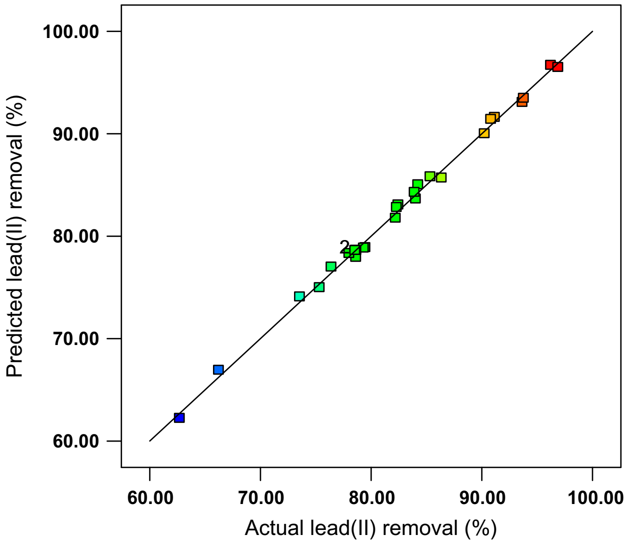

Fig. 3. The actual and predicted plot of adsorption of lead (II).

Table 4
ANOVA for response surface quadratic model for the adsorption of lead (II)

Source	Sum of squares	Degree of freedom	Mean square	*F* value	Prob > *F*	Remarks
Model	1,843.84	14	131.70	308.74	<0.0001	significant
X_1	126.46	1	126.46	296.44	<0.0001	significant
X_2	210.87	1	210.87	494.31	<0.0001	significant
X_3	170.85	1	170.85	400.49	<0.0001	significant
X_4	205.10	1	205.10	480.78	<0.0001	significant
X_1X_2	0.42	1	0.42	0.98	0.3368	
X_1X_3	38.05	1	38.05	89.19	<0.0001	significant
X_1X_4	17.27	1	17.27	40.48	<0.0001	significant
X_2X_3	98.69	1	98.69	231.35	<0.0001	significant
X_2X_4	120.77	1	120.77	283.10	<0.0001	significant
X_3X_4	114.48	1	114.48	268.35	<0.0001	significant
X_1^2	180.46	1	180.46	423.04	<0.0001	significant
X_2^2	187.56	1	187.56	439.68	<0.0001	significant
X_3^2	269.12	1	269.12	630.87	<0.0001	significant
X_4^2	52.68	1	52.68	123.49	<0.0001	significant
Residual	6.40	15	0.43	–	–	
Lack of fit	6.39	10	0.64	420.88	<0.0001	significant
Pure error	7.59E−003	5	1.59E−003	–	–	
Correlation total	1,850.24	29	–	–	–	

predicted values are evaluated from the model and are generated using the approximating functions. In Fig. 3, the values of R^2 and R^2_{adj} were found to be 0.996 and 0.993, respectively. The fair correlation coefficients might have resulted by the insignificant terms in Table 4, and most likely due to four different variables selected in wide ranges with a limited number of experiments as well as the nonlinear influence of the investigated parameters on process response.

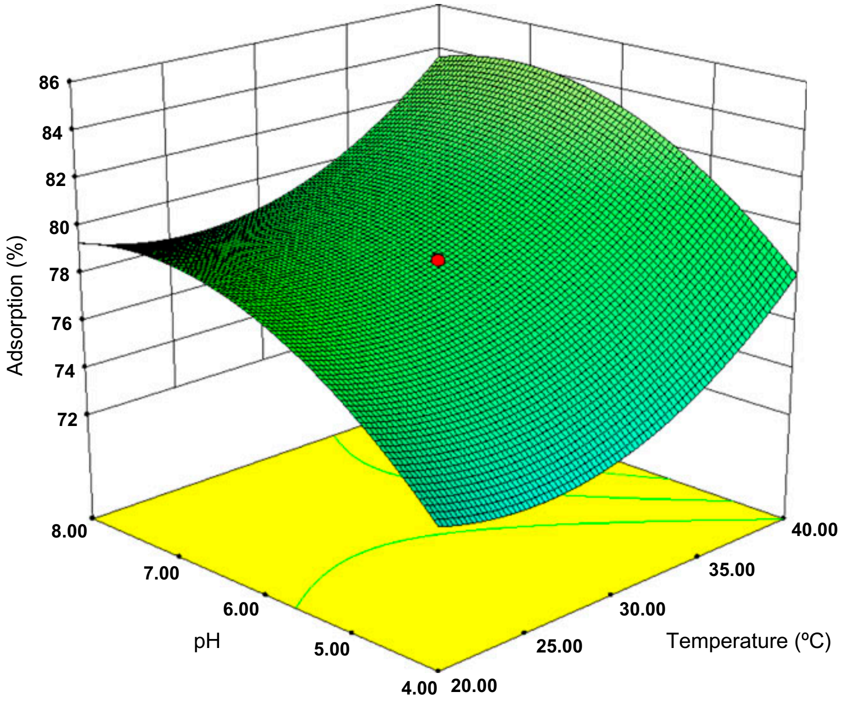

Fig. 4. The combined effect of temperature and pH on adsorption of lead (II) at constant initial concentration of lead (II) (30 mg L^{-1}) and adsorbent dose (3 g L^{-1}).

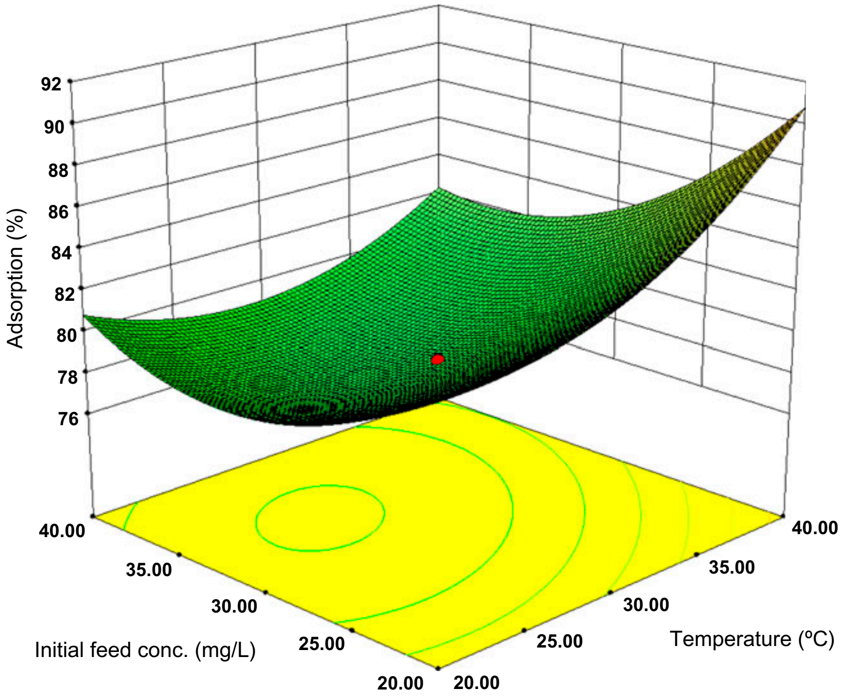

Fig. 5. The combined effect of temperature and initial concentration of lead (II) on adsorption of lead (II) at constant pH (6) and adsorbent dose (3 g L^{-1}).

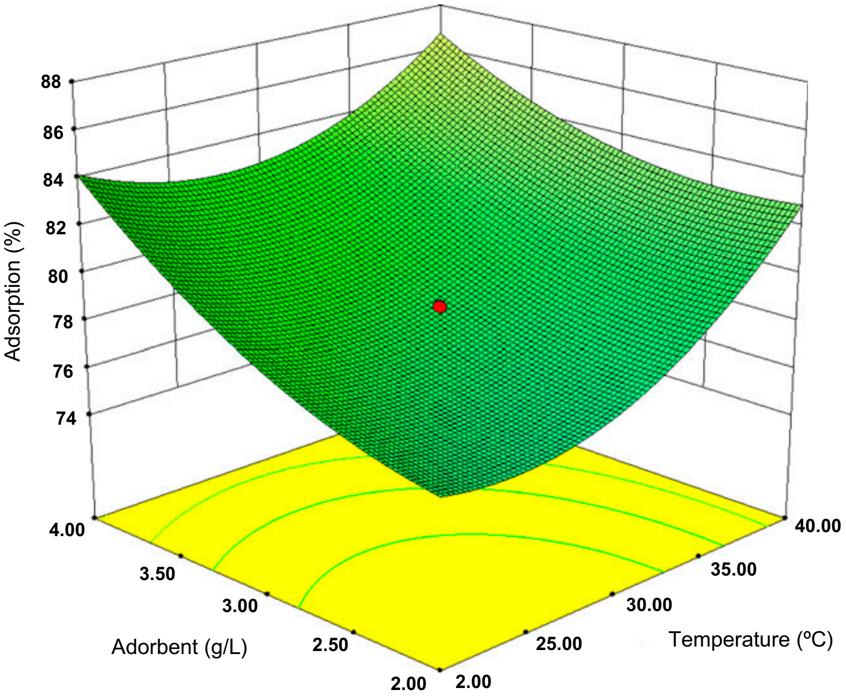

Fig. 6. The combined effect of temperature and adsorbent dose on adsorption of lead (II) at constant pH (6) and initial concentration of lead (II) (30 mg L^{-1}).

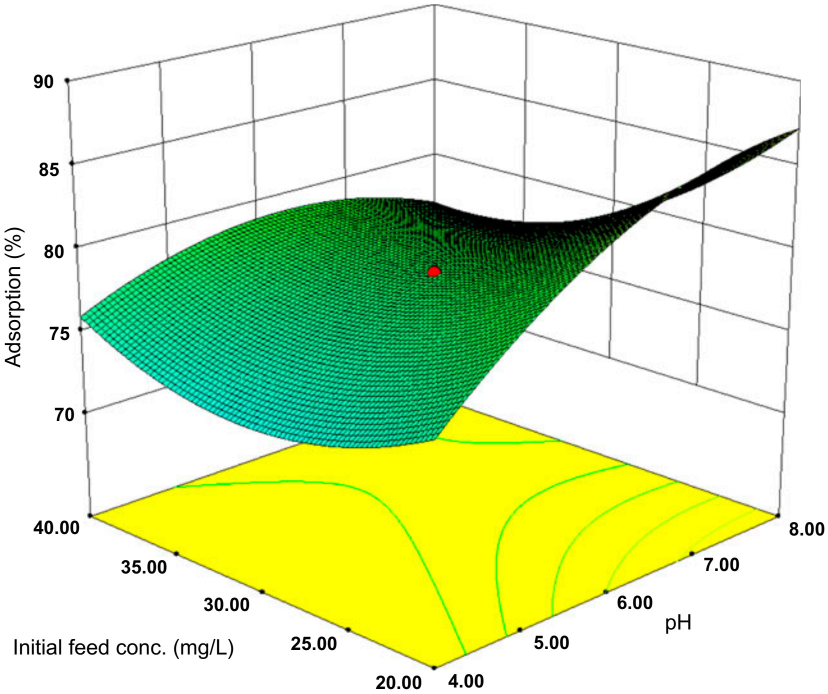

Fig. 7. The combined effect of initial concentration of Pb(II) and pH on adsorption of lead (II) at constant adsorbent dose (3 g L^{-1}) and temperature (30°C).

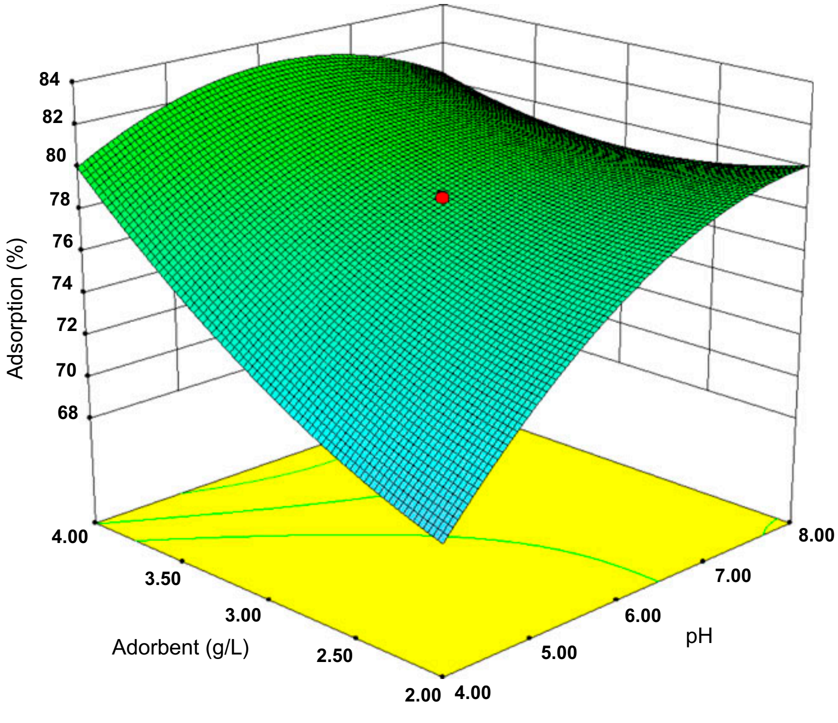

Fig. 8. The combined effect of pH and adsorbent dose on adsorption of lead (II) at constant temperature (30°C) and initial concentration of lead (II) (30 mg L^{-1}).

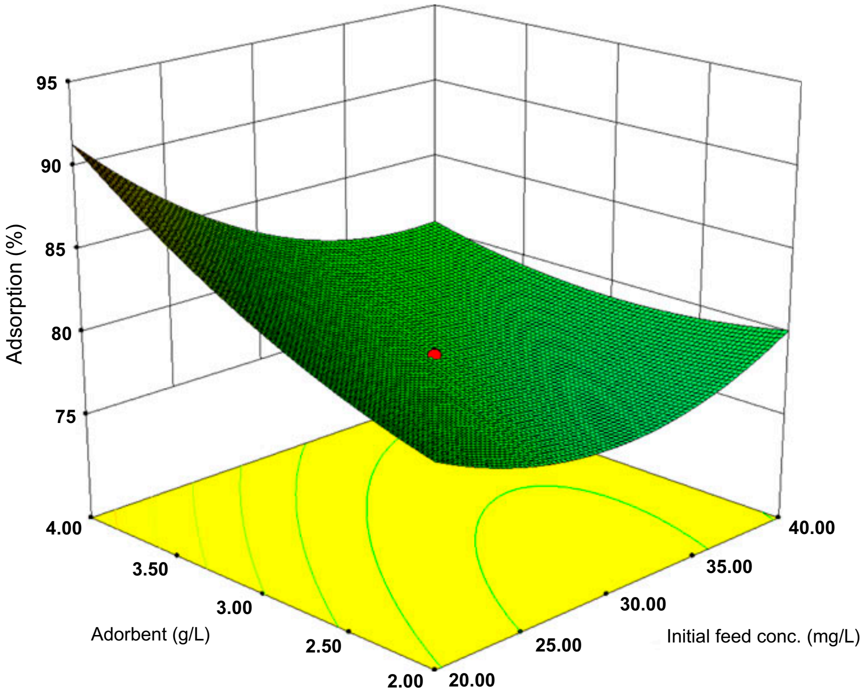

Fig. 9. The combined effect of initial concentration of lead (II) and adsorbent dose on adsorption of lead (II) at constant pH (6) and temperature (30℃).

3.3. Adsorption capacity of lead (II)

To investigate the effects of the four factors on the adsorption of lead, the RSM was used, and three-dimensional plots were drawn. Based on the ANOVA results obtained, adsorbent dose and pH were found to have significant effects on the adsorption of lead, with adsorbent dose imposing the greatest effect on the adsorption of lead (II). Initial feed concentration of lead (II) and temperature on the other hand imposed the least effect on the response. The interaction effects between X_1X_4 are considered moderate. The adsorption of lead (II) percent response surface graphs is shown in Figs. 4–9.

Fig. 4 shows the three-dimensional response surfaces, the combined effect of temperatures and pH on adsorption of lead (II) at constant initial feed concentration of lead (II) (30 mg L^{-1}) and adsorbent dose (3 g L^{-1}). Increasing the temperatures from 25 to 45℃ facilitated the removal of lead (II) ions. The increase in metal uptake with increasing temperatures may be due to either higher affinity of sites for metal or an increase in number of binding sited on activated carbon. It is clear from Fig. 4 that the percent adsorption of lead (II) decreases with increase in pH from 2 to 6 and after pH 5.65 (natural pH) no adsorption takes place at all. It is important that the maximum adsorption at all the concentrations takes place at pH 2. A maximum adsorption of lead (II) >84% was determined at constant initial feed concentration of lead (II) (30 mg L^{-1}) and adsorbent dose (3 g L^{-1}).

Fig. 5 observes the interactive effect of temperatures and initial feed concentrations of lead (II) of the solution on percent adsorption of lead (II) onto activated carbon. It shows that adsorption forward with increas-

Table 5
Model validation

Temperature, X_1 (℃)	pH, X_2	Initial feed concentration, X_3 (mg L^{-1})	Adsorbent dose, X_4 (g L^{-1})	Adsorption of Pb(II), Y (%)	
				Predicted	Experimental
50	4.07	49.10	1.44	99.28	98.82

ing metal concentrations up to 25–30 mg L^{-1} and afterward shows a slight decrease. A maximum adsorption of lead (II) >93% was determined at constant pH (6) and adsorbent dose (3 g L^{-1}). The combined effect of temperatures and initial feed concentrations of lead (II) on adsorption of lead (II) at constant pH (6) and adsorbent dose (3 g L^{-1}) are shown in Fig. 6, the three-dimensional response surfaces. A maximum adsorption of lead (II) >86% was determined at constant pH (6) and adsorbent dose (3 g L^{-1}).

The three-dimensional response surfaces of the combined effect of initial concentrations of lead (II) and pH on adsorption of lead (II) at constant adsorbent dose (3 g L^{-1}) and temperature (30˚C) are shown in Fig. 7. A maximum adsorption of lead (II) >86% was determined at constant adsorbent dose (3 g L^{-1}) and temperature (30˚C). Fig. 8 shows the three-dimensional response surfaces which were constructed to show the most important two variables (pH and adsorbent doses) on the adsorption of lead (II) at constant temperature (30˚C) and initial concentration of lead (II) (30 mg L^{-1}). It can be seen from the figure that initially the percentage removal increases very sharply with the increase in adsorbent dosages but beyond a certain value 2.5–3.0 g L^{-1}, the percentage removal reaches almost a constant value. The trend is expected because as the adsorbent doses increases the number adsorbent particles increases and thus more lead (II) is attached to their surfaces. A maximum adsorption of lead (II) >83% was determined at constant temperature (30˚C) and initial concentration of lead (II) (30 mg L^{-1}).

It can be observed from Fig. 9, the combined effect of initial feed concentrations of lead (II) and adsorbent doses on adsorption of lead (II) at constant pH (6) and temperature (30˚C), the maximum adsorption of lead (II) >91% was determined at constant pH (6) and temperature (30˚C).

3.4. Optimization by response surface modeling

One of the main aims was to find the optimum process parameters to maximize the adsorption of lead (II), from the mathematical model equations developed in the study. The quadratic model equation was optimized using quadratic programming to maximize of adsorption of lead (II) within the experimental range studied. The optimum adsorption conditions (Table 5) were determined as temperature 50˚C, initial feed concentration of lead (II) 49.10 mg L^{-1}, pH 4.07, and adsorbent dose 1.44 g L^{-1} have been determined as optimum levels of the process parameters to achieve the maximum adsorption of lead of 99.28%, compared to 98.82% which was maximum adsorption of lead (II) in the tests conducted.

4. Conclusions

The objective of the present study was to find out and optimize the lead (II) adsorption capacity of a new adsorbent activated tamarind wood. The RSM based on four variables CCD was used to determine the effect of temperature (ranging 10–50˚C), pH (ranging 2–10), initial feed concentration of lead (II) (ranging 10–50 mg L^{-1}), and adsorbent dose (ranging 1–5 g L^{-1}) on the adsorption of lead (II). The regression analysis, statistical significance, and response surface were done using Design Expert Software for predicting the responses in all experimental regions. Models were developed to correlate the adsorption variables to the responses. Through analysis of the response surfaces derived from the models, adsorbent dose was found to have the most significant effect on adsorption of lead (II). Process optimization was carried out, and the experimental values obtained for the adsorption of lead are found to agree satisfactorily with the values predicted by the models. The optimal adsorption of lead was obtained adsorbent dose, temperature, initial concentration of lead (II), and initial pH of the lead (II) solution were found to be 1.44 g L^{-1}, 50˚C, 49.10 mg L^{-1} and 4.07, respectively, resulting in 99.28% of adsorption of lead (II). Furthermore, the study revealed that owing to the high initial feed concentration of lead (II) the optimum adsorption is achieved at different process parameters. However, more investigations are needed on different types of industrial wastewaters, continuous process, and different operating conditions before such conclusions can be generalized.

References

[1] R. Jalali, H. Ghafourian, Y. Asef, S.J. Davarpanah, S. Sepehr, Removal and recovery of lead using nonliving biomass of marine algae, J. Hazard. Mater. 92 (2002) 253–262.

[2] V.K. Gupta, M. Gupta, S. Sharma, Process development for the removal of lead and chromium from aqueous solutions using red mud—An aluminium industry waste, Water Res. 35(5) (2001) 1125–1134.

[3] K. Conrad, H.C. Bruunhansen, Sorption of zinc and lead on coir, Bioresour. Technol. 98(1) (2007) 89–97.

[4] M. Nadeem, R. Nadeem, H.U. Nadeem, S.S. Shah, Accumulation of lead and cadmium in different organs of chicken, Pakistan J. Sci. Res. 57(1–2) (2005) 71–76.

[5] World Health Organization, Guidelines for Drinking Water Quality, vol. 1–2, World Health Organization, Geneva, 1984.

[6] A. Groffman, S. Peterson, D. Brookins, Removing lead from wastewater using zeolites, Water Environ. Technol. 5 (1992) 54–59.

[7] ISI, Tolerance limits for industrial effluents prescribed by Indian Standards Institution, IS: 2490 (Part II), New Delhi, 1982.

[8] ISI, Drinking water specification prescribed by Indian Standards Institution, IS: 10500, New Delhi, 1991.

[9] M.M. Husein, J.H. Vera, M.E. Weber, Removal of lead from aqueous solutions with sodium caprate, Sep. Sci. Technol. 33(12) (1998) 1889–1904.

[10] S.W. Lin, R.M.F. Navarro, An innovative method for removing Hg^{2+} and Pb^{2+} in ppm concentrations from aqueous media, Chemosphere 39(11) (1999) 1809–1817.

[11] D. Petruzzelli, M. Pagano, G. Tiravanti, R. Passino, Lead removal and recovery from battery wastewaters by natural zeolite clinoptilolite, Solvent Extr. Ion Exch. 17(3) (1999) 677–694.

[12] A. Saeed, M. Iqbal, M.W. Akhtar, Removal and recovery of lead(II) from single and multimetal (Cd, Cu, Ni, Zn) solutions by crop milling waste (black gram husk), J. Hazard. Mater. 117(1) (2005) 65–73.

[13] S. Doyurum, A. Çelik, Pb(II) and Cd(II) removal from aqueous solutions by olive cake, J. Hazard. Mater. 138 (1) (2006) 22–28.

[14] C.P. Dwivedi, J.N. Sahu, C.R. Mohanty, B.R. Mohan, B.C. Meikap, Column performance of granular activated carbon packed bed for Pb(II) removal, J. Hazard. Mater. 156(1–3) (2008) 596–603.

[15] C.K. Singh, J.N. Sahu, K.K. Mahalik, C.R. Mohanty, B.R. Mohan, B.C. Meikap, Studies on the removal of Pb(II) from wastewater by activated carbon developed from Tamarind wood activated with sulphuric acid, J. Hazard. Mater. 153 (2008) 221–228.

[16] J.N. Sahu, S. Agarwal, B.C. Meikap, M.N. Biswas, Performance of a modified multi-stage bubble column reactor for lead(II) and biological oxygen demand removal from wastewater using activated rice husk, J. Hazard. Mater. 161 (2009) 317–324.

[17] J. Goel, K. Kadirvelu, C. Rajagopal, V. Kumar Garg, Removal of lead(II) by adsorption using treated granular activated carbon: Batch and column studies, J. Hazard. Mater. 125 (2005) 211–220.

[18] G. Issabayeva, M.K. Aroua, N.M.N. Sulaiman, Removal of lead from aqueous solutions on palm shell activated carbon, Bioresour. Technol. 97(18) (2006) 2350–2355.

[19] J. Acharya, J.N. Sahu, C.R. Mohanty, B.C. Meikap, Removal of lead(II) from wastewater by activated carbon developed from Tamarind wood by zinc chloride activation, Chem. Eng. J. 149 (2009) 249–262.

[20] A.C. Lua, J. Guo, Chars pyrolyzed from oil palm wastes for activated carbon preparation, J. Environ. Eng. (1999) 72–76.

[21] M.G. Lussier, J.C. Shull, D.J. Miller, Activated carbon from cherry stones, Carbon 32(8) (1994) 1493–1498.

[22] W. Su, L. Zhou, Y. Zhou, Preparation of microporous activated carbon from coconut shells without activating agents, Letters to the Editor, Carbon 41(4) (2003) 861–863.

[23] C.J. Kirubakaran, K. Krishnaiah, S.K. Seshadri, Experimental study of the production of activated carbon from coconut shells in a fluidized bed reactor, Ind. Eng. Chem. Res. 30(11) (1991) 2411–2416.

[24] D. Mohan, K.P. Singh, Single- and multi-component adsorption of cadmium and zinc using activated carbon derived from bagasse—An agricultural waste, Water Res. 36(9) (2002) 2304–2318.

[25] J.W. Kim, M.H. Sohn, D.S. Kim, S.M. Sohn, Y.S. Kwon, Production of granular activated carbon from waste walnut shell and its adsorption characteristics for Cu^{2+} ion, J. Hazard. Mater. 85 (2001) 301–315.

[26] S. Ricordel, S. Taha, I. Cisse, G. Dorange, Heavy metals removal by adsorption onto peanut husks carbon: Characterization, kinetic study and modeling, Sep. Purif. Technol. 24(3) (2001) 389–401.

[27] C. Namasivayam, D. Sangeetha, Equilibrium and kinetic studies of adsorption of phosphate onto $ZnCl_2$ activated coir pith carbon, J. Colloid Interface Sci. 280 (2004) 359–365.

[28] K. Kadirvelu, K. Thamaraiselvi, C. Namasivayam, Adsorption of nickel(II) from aqueous solution onto activated carbon prepared from coirpith, Sep. Purif. Technol. 24(3) (2001) 497–505.

[29] M. Moyo, L. Chikazaza, B.C. Nyamunda, U. Guyo, Adsorption batch studies on the removal of Pb(II) using maize tassel based activated carbon, J. Chem. 2013 (2013) 1–8.

[30] P. Mohanty, S. Majhi, J.N. Sahu, K.K. Pant, Response surface modeling and optimization of CO hydrogenation for higher liquid hydrocarbon using Cu–Co–Cr+ ZSM-5 bifunctional catalyst, Ind. Eng. Chem. Res. 51 (13) (2012) 4843–4853.

[31] S. Pradhan, C.S. Madankar, P. Mohanty, S.N. Naik, Optimization of reactive extraction of castor seed to produce biodiesel using response surface methodology, Fuel 97 (2012) 848–855.

[32] S. Majhi, P. Mohanty, A.K. Dalai, K.K. Pant, Statistical optimization of process variables for methane conversion over Zn–Mo/H-ZSM-5 catalysts in the presence of methanol, Energy Tech. 1(2–3) (2013) 157–165.

[33] J.N. Sahu, J. Acharya, B.C. Meikap, Response surface modeling and optimization of chromium(VI) removal from aqueous solution using tamarind wood activated carbon in batch process, J. Hazard. Mater. 172 (2009) 818–825.

[34] Z. Alam, S.A. Muyibi, J. Toramae, Statistical optimization of adsorption processes for removal of 2,4-dichlorophenol by activated carbon derived from oil palm empty fruit bunches, J. Environ. Sci. 19 (2007) 674–677.

[35] D.C. Montgomery, Design and Analysis of Experiments, fifth ed., John Wiley and Sons, New York, NY, 2001.

[36] R.H. Myers, Response Surface Methodology, Allyn and Bacon, New York, NY, 1971.

[37] V. Gunaraj, N. Murugan, Application of response surface methodology for predicting weld bead quality in submerged arc welding of pipes, J. Mater. Process. Technol. 88 (1999) 266–275.

[38] G.E.P. Box, J.S. Hunter, Multi-factor experimental design for exploring response surfaces, Ann. Math. Stat. 28 (1957) 195–241.

[39] G.E.P. Box, W.G. Hunter, The 2^{k-p} fractional factorial designs, parts I and II, J. Technometr. 3 (1961) 311–458.

[40] T.J. Napier-Munn, The Central Composite Rotatable Design JKMRC, The University of Queensland, Brisbane, 2000.

[41] G.E.P. Box, W.G. Hunter, Statistics for Experiments: An Introduction to Design. Data Analysis and Model Building, Wiley Interscience, New York, NY, 1987.

[42] R.H. Myers, D.C. Montgomery, Response Surface Methodology: Process and Product Optimization Using Designed Experiments, second ed., John Wiley and Sons, New York, NY, 2002.